

Signatures of Enhanced Superconducting Properties in Niobium Cavities

D. Bafia,^{1,*} A. Grassellino,¹ M. Checchin,² J. F. Zasadzinski,³ and A. Romanenko¹

¹Fermi National Accelerator Laboratory, Batavia, Illinois 60510, USA

²SLAC National Accelerator Laboratory, Menlo Park, California 94025, USA

³Department of Physics, Illinois Institute of Technology, Chicago, Illinois 60616, USA

(Dated: January 16, 2025)

Superconducting radio-frequency (SRF) niobium cavities are critical for modern particle accelerators, as well as for advancing superconducting quantum systems and enabling ultra-sensitive searches for new physics. In this work, we report a systematic observation of an anomalous frequency dip in Nb cavities, which occurs at temperatures just below the critical temperature (T_c), indicative of enhanced superconducting properties at $T \ll T_c$. The magnitude of this dip is strongly correlated with the RF surface resistance, impurity distribution near the surface, and T_c . We also present the first demonstration of the coherence peak in the AC conductivity of Nb SRF cavities. By comparing recent theories developed to model this experimental data, we show that the frequency dip feature, larger coherence peak height, and reduction in the temperature-dependent surface resistance with RF current occur at minimal but finite levels of disorder.

I. INTRODUCTION

Superconducting radio frequency (SRF) niobium cavities are record-high quality factor $Q_0 > 10^{10} - 10^{11}$ man-made resonators that serve as the primary accelerating structures in modern particle accelerators [1], longest coherence microwave quantum superconducting systems [2], and an ultrasensitive platform for dark sector and dark matter candidate searches [3–6]. These ultra-high quality factors are enabled by the low microwave surface resistance R_s ($\propto 1/Q_0$) of superconducting Nb. Typically, R_s increases with the magnitude of the peak surface magnetic field B_p due to increased screening currents. Extensive research over the past decades has allowed the discovery and mitigation of several such field-dependent physical mechanisms in various regimes [1]. This most recently includes proximity-coupled niobium nanohydrides [7] and their mitigation by oxygen inward diffusion [8] and the reduction of two-level system-driven dissipation by oxide removal [2, 9].

This steady improvement has revealed new SRF phenomena that remain poorly understood, most notably the factor of four increase in Q_0 and the field-dependent *increase* in the quality factor of nitrogen-doped [10] cavities, which is commonly referred to as the positive slope Q. The unusual effect stems from an anomalous decrease in the temperature-dependent component of the surface resistance R_T with increasing field [10]. In essence, it is as if superconducting pairing strengthens with an increased RF field and current. Material studies have highlighted its dependence on the concentration and distribution of nitrogen in the vicinity of the surface. Possible mechanisms include a field-stimulated smearing of the BCS density of states [11, 12], anomalous skin effects [13], and the field-driven nonequilibrium redistribution of thermally excited quasiparticles to higher energy levels [14]. Still, a systematic study of the effect of doping

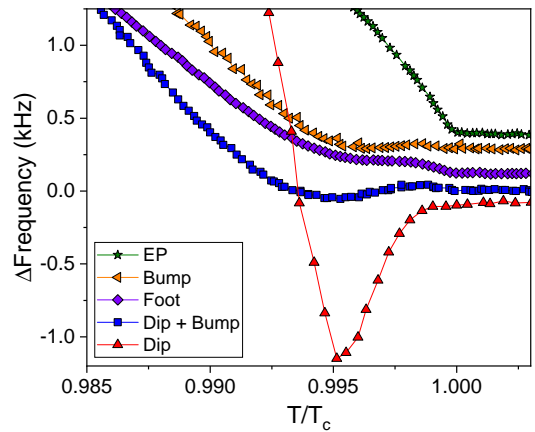


FIG. 1. Five observed resonant frequency variations of 1.3 GHz elliptical niobium SRF cavities near T_c . Each frequency curve has been offset for clarity.

on quasiparticle lifetimes and density of states as well as strong coupling pairing effects in SRF cavities has not been reported and is critical for the understanding of the effect.

While many studies have focused on the quality factor and surface resistance, here we report that the cavity resonant frequency provides another valuable avenue for gaining insight into the underlying physical phenomena, as its changes are directly connected to the properties of the superconducting condensate. We find the existence of anomalous frequency features just below the critical transition temperature T_c of the bulk superconducting Nb. Fig. 1 shows the five resonant frequency variations just below the critical transition temperature (T_c) in Nb SRF cavities. All five features have been observed at low fields (< 1 mT) while warming and cooling through T_c , which is expected as the superconducting phase transition is of the second order.

The AC complex conductivity enables further insight on quasiparticles and superconducting carriers. For fre-

* dbafia@fnal.gov

quencies far below the superconducting gap ($\hbar\omega \ll \Delta$), σ_1 exhibits the coherence peak, a nonmonotonic dependence of the quasiparticle conductivity with temperature that arises due to coherence factors in BCS theory [15] and is analogous to the Hebel-Slichter peak in nuclear spin relaxation [16]. However, until now, this coherence peak has not been reported in Nb SRF cavities. We show that the height of the coherence peak also correlates with the frequency dip in Fig.1.

In this article, a systematic study is presented on a large number (>40) of bulk niobium SRF cavities revealing the anomalous decrease (dip) in cavity resonant frequency at temperatures just below T_c in nitrogen-doped cavities. In addition, we report that the other four (non-dip) characteristic temperature dependencies uniquely correspond to other explored surface treatments, and thus correlate strongly with cavity performance in R_T with the stored field. The measured coherence peak in the complex conductivity of bulk niobium SRF cavities is fitted with a phenomenological model incorporating a pair-breaking term in the BCS [15] density of states. We comment on different models proposed by other groups which help provide insight on the origins of these various phenomena. Fits with theories suggest that the coherence peak, along with the dip phenomenon, high Q_0 , and R_T decrease with field, are signatures of improved superconducting properties and occur when extrinsic pair-breaking scattering and pair-conserving scattering from nonmagnetic impurities are minimal but finite.

II. EXPERIMENTAL PROCEDURE

A large set of bulk niobium SRF cavities of TESLA [17] elliptical shape were employed for our studies. The resonant frequencies of these cavities varied from 650 MHz to 3.9 GHz, which allowed probing the low frequency limit of Nb ($\hbar\omega \ll \Delta$). All cavities went through a bulk electropolishing of 120 μm material removal and 800°C hydrogen degassing step [18] followed by various surface treatments. These treatments included ~ 40 μm electropolishing (referred to as EP here), nitrogen infusion [19], 120°C baking for 48 hours [20], 75/120°C baking [21, 22] wherein cavities were first baked at 75°C before the standard 120°C bake, and nitrogen doping [10] with varying dopant concentrations. Dopant concentration is varied by altering the durations of baking in N atmosphere and in vacuum, which has the shorthand notation of minutes in N/minutes in vacuum (i.e., 2/6) and/or the amount of removal *via* EP.

All cavities were first cooled down to 2 K where standard measurements [23] of Q_0 as a function of the peak surface magnetic field B_{peak} have been performed. To extract R_T from the measured Q_0 , we used the methods laid out in [14].

Measurements of the resonant frequency f_0 with temperature were made as follows. Cavities were equipped with resistance temperature detectors (RTDs), placed in

a helium dewar, and pre-cooled to 4.2 K. We used heaters located at the bottom of dewar to boil off the liquid helium and facilitate warming. This procedure allowed for a warming rate of < 0.1 K/min, ensuring thermalization of the cavity, as confirmed by the RTD readings. Resonant frequency was recorded with a vector network analyzer (VNA). Measurements persisted through the niobium superconducting transition temperature at ~ 9.2 K. After measurements, the data was corrected to account for variations in dewar gas pressure.

For several $f_0(T)$ datasets, an effective mean free path ℓ within the cavity surface layer has been obtained by converting the measured frequency shift with temperature near T_c into a shift in the magnetic field penetration depth $\lambda(T)$ using Slater's theorem [24] and fitting based on the modified Halbritter routine [25], following the same technique outlined in [26].

To calculate the AC conductivity, we used the method utilized by Trunin *et al.* [27]. To extract the surface resistance, we measured Q_0 from 1.5 K up to 10 K using a combination of standard power balance measurements in continuous wave and decay modes along with VNA measurements. We converted to surface resistance *via* $R_s = G/Q_0$, where $G = 270 \Omega$. The surface reactance was measured utilizing the above discussed frequency vs temperature measurements from 6 K to 10 K and extrapolating to lower temperatures by means of fitting with the Halbritter routine [25] and using $X_s(T) = -2G\Delta f_0(T)/f_0 + X_n$. We obtained the additive constant using the normal conducting surface resistance measured just above the transition temperature $R_n(10 \text{ K})$. In the local limit, valid for dirty Nb, $R_n(10 \text{ K}) = X_n(10 \text{ K})$. When the local limit is not applicable, as is true for high purity niobium [20], the correct relationship between R_s and X_s is obtained using the universal impedance curves plotted against the dimensionless parameter α calculated by Reuter and Sondheimer in the microwave region [28]. The parameter α is proportional to $\ell^3/\rho\ell$, where ℓ is the mean free path and $\rho\ell$ is a temperature independent material constant, which is $6 \times 10^{-16} \Omega\text{m}^2$ for Nb [20]. Finally, the complex conductivity is calculated as

$$\sigma = \sigma_1 + i\sigma_2 = \omega\mu_0 \left(\frac{2R_s X_s}{(R_s^2 + X_s^2)^2} + i \frac{X_s^2 - R_s^2}{(R_s^2 + X_s^2)^2} \right). \quad (1)$$

III. RESULTS

A. Effect of Impurity Structure on Frequency Variations Near T_c

Overall, we have studied the frequency response of 41 cavities with various impurity structures in the RF layer. Of these 41, we find a clear dip in the resonant frequency just below the T_c in 22 N-doped cavities, similar to what is observed in Fig. 1. For other treatments, we observed the four other characteristic behaviors.

	N-doped	N-Infused	75/120°C	120°C	EP
Dip	22		1 ^a		
Foot		1	5		
Bump			1		
Dip+Bump		2			1
Standard		1	3	2	2

^a $\Delta f_{dip} < 50$ Hz as compared to ~ 1 -2 kHz in doped cavities, likely an artifact of the pressure correction

TABLE I. Occurrence of features in $f_0(T)$ data near T_c for five typical SRF cavity surface treatments.

B. Effect of MFP on Frequency Dip Feature

To investigate the dependence of the dip on the nitrogen concentration, one cavity subjected to 3/60 nitrogen doping underwent several sequential material removal steps of the RF surface *via* EP, with RF measurements performed after each step. The material removal allowed to gradually decrease the concentration of N present in the RF layer, resulting in an increase in ℓ . After the combined 30 μm material removal, the cavity was bulk electropolished and re-processed with the 2/6 N-doping surface treatment. The $R_T(B_{\text{peak}})$ and $f_0(T)$ results along with the corresponding material removal amounts and extracted ℓ values are presented in Fig. 2.

We observe that dilute and uniform concentrations of nitrogen (short ℓ) produce a characteristic decrease in R_T at higher B_{peak} , a weak suppression in T_c , and an anomalous frequency dip just before T_c . As nitrogen concentration gradually decreases with more material removal, these behaviors are gradually diminished. The R_T behavior with field approaches that of a typical EP cavity. Meanwhile, the dip magnitude diminishes as the transition temperature assumes the clean niobium value. Subsequent bulk electropolishing and 2/6 doping, which is known to produce a larger nitrogen concentration than 3/60 doping, shows a return of the dip feature with a larger magnitude and lower T_c .

Fig. 2(c) plots the dip magnitude and transition temperature against ℓ . The dip magnitude decreases strongly (close to exponentially) while the transition temperature increases with increasing ℓ values. The T_c varies by ~ 120 mK throughout the course of the study, which is in good agreement with previous work on the effects of nitrogen and oxygen on niobium T_c [29]. Possible origins for this T_c suppression in the presence of N interstitial may stem from lattice parameter expansion [29] or Fermi surface anisotropy [30]. Our findings clearly show that a frequency dip and corresponding T_c suppression occur in the presence of uniform and dilute concentrations of N impurities and that impurity concentration serves as a critical parameter in determining the extent of the phenomena.

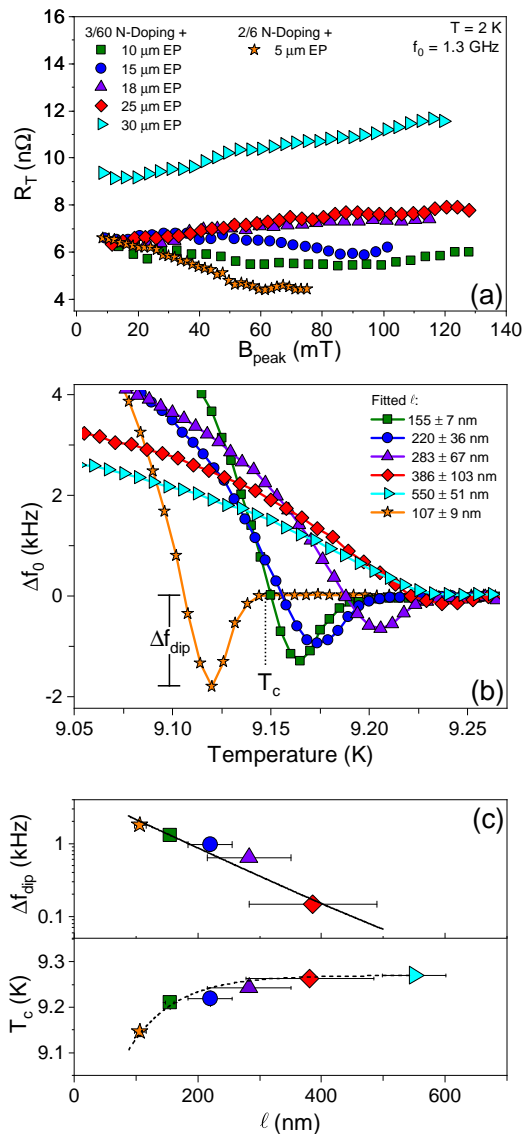


FIG. 2. (a) Temperature dependent surface resistance at 2 K with peak magnetic field and (b) resonant frequency response with temperature of a single 1.3 GHz Nb cavity after sequential removal of the surface post nitrogen doping. The legend in (b) presents the fitted ℓ in the RF layer after each step. Resonant frequency shift is reported relative to the normal conducting value near 10 K. The parameter Δf_{dip} is called the dip magnitude. (c) Dip magnitude and T_c are plotted against the fitted ℓ . Horizontal error bars come from fitting; vertical error bars are smaller than the data points. Solid and dashed lines show $e^{-\ell}$ and $-e^{-\ell}$ relationships, respectively.

C. Correlating Q_0 with Δf_{dip}

The evolution observed in Fig. 2 suggests correlation between the frequency dip and Q_0 ($\propto 1/R_s$); to investigate this, we plotted the quality factor measured at 68 mT against the dip magnitude for an ensemble of variously nitrogen doped cavities in Fig. 3. Indeed, we ob-

serve a linear trend, suggesting a potential relationship between the positive Q -slope and frequency dip phenomena. We note that the trend shown in Fig. 3 is relevant for the accelerator community as it facilitates a method for quickly estimating the quality factor of N-doped cavities at high fields from low field frequency domain measurements, which may be practical when high power infrastructure is not readily available.

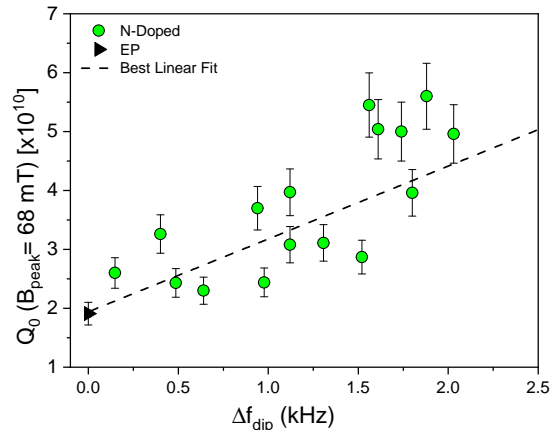


FIG. 3. Quality factor measured at 68 mT and a temperature of 2 K plotted against the dip magnitude for variously nitrogen doped cavities. Shown for reference are results obtained from a cavity post EP.

D. Effect of Resonant Frequency on Dip

To study the effect of resonant frequency on the dip, four niobium cavities with $f_0=650$ MHz, 1.3 GHz, 2.6 GHz, and 3.9 GHz were subjected to the same 2/6 N-doping surface treatment, producing an identical impurity structure in each cavity. The results are shown in Fig. 4(a). We observe that resonant frequency is linearly related with the dip magnitude, as shown in Fig. 4(b). Furthermore, the degree of R_T reversal, defined here as the negative of the slope from 15 mT to 64 mT of the $R_T(B_{\text{peak}}, T = 2 \text{ K})$ curve normalized to the value at 15 mT, also exhibits a linear trend with the resonant frequency. A similar dependence of the R_T reversal is shown in [14] where it is hypothesized that such behavior may be driven by non-equilibrium superconductivity.

E. Measurement of AC Complex Conductivity

To gain insight on the conditions under which different frequency features near T_c occur, we measured the AC complex conductivity of two niobium cavities: i) the cavity presented in Fig. 2(a) with $\ell = 550 \pm 51$ nm which showed the standard feature near T_c (which we call the EP cavity) and ii) and a cavity post nitrogen doping which exhibited the prominent dip. Fig. 5(a) and its inset

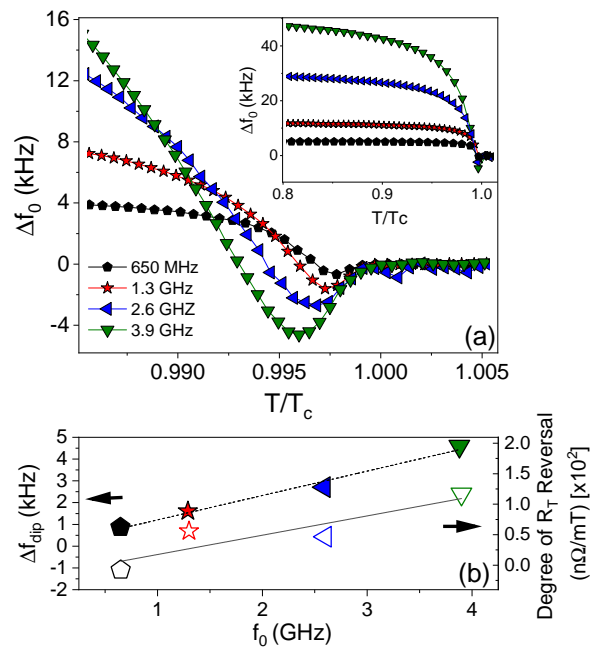


FIG. 4. (a) Frequency response with temperature of four cavities, each with different resonant frequency, processed to yield an identical nitrogen concentration in the RF layer. Inset shows the response over a larger range of temperatures. (b) Left-hand axis shows the dip magnitude plotted against the fundamental resonant frequency for each cavity. The right-hand axis plots the degree of reversal of the temperature dependent component of the surface resistance for each cavity, as defined in the text. Dashed and solid lines show linear fits.

shows the expected $Q_0(B_p)$ and $R_T(B_p)$ behaviors characteristic of cavities subjected to these surface treatment. Fig. 5(b) presents the real and the imaginary parts of the measure surface impedance of the two cavities. For the N-doped cavity, the transition temperature was 9.04 K; using Fig. 2(c), the extrapolated ℓ was about 70 nm.

To confirm the validity of our measured reactance, we calculated the experimental penetration depth at $T = 0 \text{ K}$ via $X_{s,0} = \omega\mu_0\lambda_{0,\text{exp}}$ using the Halbritter routine to extrapolate data to 0 K and compared with the effective penetration depth $\lambda_{\text{eff}} = \lambda_L(1 + \xi_0/\ell)^{1/2}$. For Nb, $\lambda_L = 39$ nm and $\xi_0 = 38$ nm [31]. The experimental and calculated results shown in Table II are in good agreement.

Treatment	$X_{s,0}$ [Ω]	ℓ [nm]	$\lambda_{0,\text{exp}}$ [nm]	λ_{eff} [nm]
EP	3.70×10^{-4}	550	36 ± 4	40
N-Doped	5.88×10^{-4}	70	57 ± 6	48

TABLE II. Comparison of experimentally and theoretically obtained values for the penetration depth at $T = 0 \text{ K}$.

The calculated AC complex conductivities of the N-doped and EP cavities are presented in Fig. 5(c). We note that as the technique used to measure the surface impedance sums over the inner RF surface, these curves represent the average cavity response.

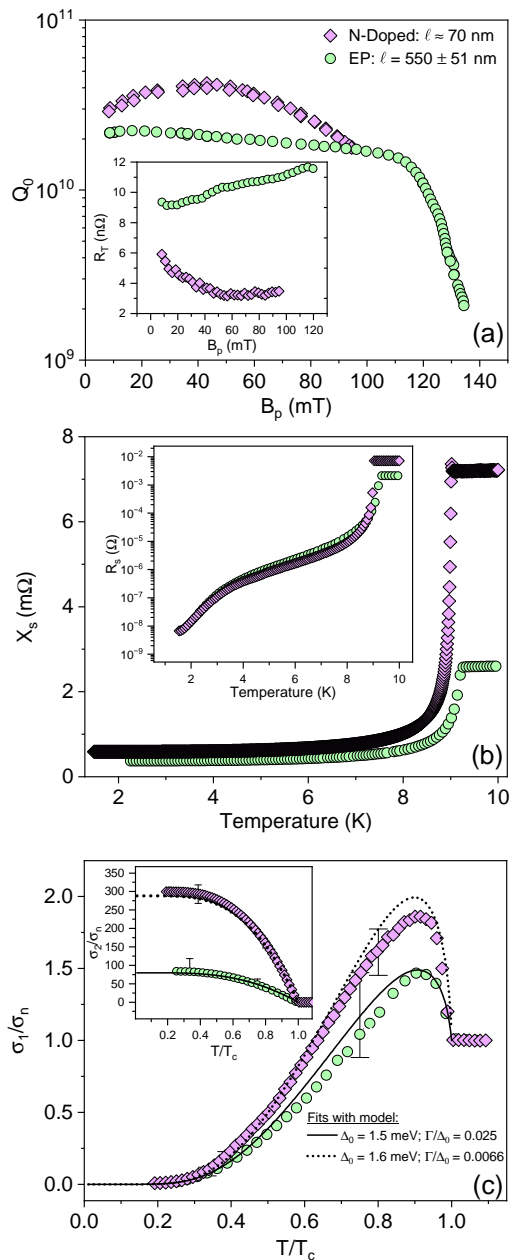


FIG. 5. (a) Quality factor vs peak magnetic field of two 1.3 GHz cavities subjected to EP or N-doping. Inset shows the temperature dependent surface resistance at 2 K as a function of peak magnetic field. (b) Surface reactance of the EP and N-doped cavities as a function of temperature; inset depicts the surface resistance as a function of temperature. (c) Real (σ_1) and imaginary (σ_2) components of the AC conductivity normalized to the normal conducting value σ_n . Error bars for the test post N-doping are dominated by measurement uncertainty while those shown post EP are dominated by error in the fitted ℓ value. Dashed and solid lines show fits.

The non-monotonic dependence in the real part of the complex conductivity in BCS superconductors, called the coherence peak, arises due to the singularity in the superconducting density of states at the gap edge [15, 32].

According to Dynes *et al.* [33], inelastic scattering smears the singularity and introduces subgap quasiparticle states. By incorporating the Dynes smearing parameter Γ into the MB conductivity, it is possible to obtain a phenomenological measure of the pair-breaking processes present in a system by fitting the coherence peak using

$$\frac{\sigma_1}{\sigma_n} = \frac{2}{\hbar\omega} \int_{\Delta}^{\infty} \frac{[f(E) - f(E + \hbar\omega)]g(E, \Gamma)}{\sqrt{(E + i\Gamma)^2 - \Delta^2}} dE + \frac{1}{\hbar\omega} \int_{\Delta - \hbar\omega}^{-\Delta} \frac{[1 - 2f(E + \hbar\omega)]g(E, \Gamma)}{\sqrt{(E + i\Gamma)^2 - \Delta^2}} dE, \quad (2)$$

$$\frac{\sigma_2}{\sigma_n} = \frac{2}{\hbar\omega} \int_{\Delta - \hbar\omega, -\Delta}^{\Delta} \frac{[1 - 2f(E + \hbar\omega)]g(E, \Gamma)}{\sqrt{(\Delta^2 - (E + i\Gamma)^2)}} dE, \quad (3)$$

$$g(E, \Gamma) = \frac{(E + i\Gamma)((E + i\Gamma) + \hbar\omega) + \Delta^2}{\sqrt{((E + i\Gamma) + \hbar\omega)^2 - \Delta^2}}. \quad (4)$$

From Fig. 5(c), we observe that both the EP and N-doped cavities exhibit the so-called coherence peak, with the maxima at $\sim 0.9 T/T_c$ differing in amplitude. This suggests a variation in the quasiparticle behavior within the RF layer due to distinct impurity distributions. Moreover, the stark difference observed in σ_2/σ_n between the two cavities highlights a variance in the superconducting condensate behavior.

The dashed and solid curves in Fig. 5(c) are calculated using Eq. 2-4. We find that both σ_1/σ_n and σ_2/σ_n of the EP cavity are best modelled with an average superconducting gap $\Delta_0 = 1.5$ meV and an inelastic scattering parameter $\Gamma/\Delta_0 = 0.025$. The N-doped cavity is instead better fitted with a larger average superconducting gap $\Delta_0 = 1.6$ meV and a lower level of pair-breaking ($\Gamma/\Delta_0 = 0.0066$). Note that a larger coherence peak occurs for the cavity with greater elastic scattering (shorter ℓ) due to the presence of N interstitial. According to Anderson's theorem [34], elastic scattering off nonmagnetic impurities has no effect on superconductivity. As a result, while N impurities increase scattering, they likely mitigate depairing processes which results in a larger coherence peak.

IV. DISCUSSION

The frequency phenomena and trends observed in this work have stimulated the development of new theories which seek to provide insight into their microscopic origins. Ueki *et al.* provided the first explanation of the anomalous near T_c frequency phenomena [35] by calculating the complex surface impedance *via* Slater's approach to solving Maxwell's equations for the case of a cavity while considering anisotropy in the superconducting gap [30] and inhomogeneous disorder within the penetration

depth. By varying the level of disorder within the cavity screening region, Ueki correctly calculated the foot, dip+bump, and dip features in the frequency response just before T_c . Moreover, the authors obtained the predicted cavity Q_0 as a function of disorder. We note that the frequency dip feature and a maximum in Q_0 were obtained for intermediate levels of disorder. Ueki also correctly reproduced the frequency dependence of the dip feature reported in Fig. 4. Zarea *et al*, instead, derived the eigenvalue equation for the fundamental TM mode of a cylindrical RF cavity which considers the current response obtained with the Keldysh formulation of the quasiclassical theory of superconductivity [36]. The result considers the confinement of the normal conducting and superconducting currents within the RF layer and shows that the anomalous frequency dip is a product of the competition between the normal metal skin depth and the London penetration depth. We note that Zarea also found that the frequency dip and a maximum in cavity Q_0 occur at intermediate levels of disorder.

Taken together, the theories by Ueki and Zarea indeed support the observation that a dilute concentration of nitrogen in Nb, which provides an intermediate level of disorder, is responsible for the anomalous frequency dip just before T_c . Moreover, they report that greater levels of disorder yield a larger dip magnitude and an increase in Q_0 toward its peak value, giving one model for the origins of the linear correlation observed in Fig. 3.

The results presented in Fig. 5 have also stimulated theoretical work by other groups which further improves our understanding of the mechanisms behind the improved performance of niobium SRF cavities in the presence of various near-surface impurity profiles. Herman and Hlubina [37] used the Nam approach [38] to calculate the optical response of a superconductor in the limit where energy tends to zero and with pair-conserving and pair-breaking elastic-scattering processes built into the energy and gap functions. The result describes the effect of subgap quasiparticle states on the optical conductivity and utilizes the concept of ‘‘Dynes superconductors.’’ The authors present excellent fits to the real and imaginary parts of the AC complex conductivity of both cavities presented in Fig. 5 and find that pair-breaking processes dominate the height of the coherence peak in σ_1/σ_n . Herman and Hlubina also highlight that the ratio between pair-breaking and pair-conserving scattering rates is key in determining the coherence peak extent and show that cleaner superconductors counterintuitively yield lower peak heights. Kubo, instead, used the Dynes Γ in the Eilenberger formalism of the BCS theory to calculate several superconductor quantities in the presence of varying levels of nonmagnetic impurity scattering rates as a function of temperature and energy [39]. These calculations also well model the results presented in Fig. 5 and, similar to Herman and Hlubina, show that the ratio between pair-breaking and nonmagnetic impurity scattering rates is key in determining the height of the coherence peak. Moreover, Kubo finds that there exists a

minimum in the surface resistance at finite levels of pair-breaking and pair-conserving scattering. We note that the phenomenologically derived Eqs. 2-4 in the present manuscript reproduce the salient feature of the above theories that greater smearing of the density of states yields a reduction of the coherence peak height and the zero-temperature value of σ_2/σ_n .

The above experimental and theoretical observation that different impurity structures in Nb yield varying RF performance due to the level of scattering within the RF surface is consistent with point contact tunneling spectroscopy (PCTS) studies by Groll *et al.* on similarly treated cavity cutouts [40]. The N-doped samples in those studies show more homogeneous Δ_0 values and lower levels of Γ/Δ_0 than those which come from EP cavities [41]. The lower level of pair-breaking scattering processes observed in Fig. 5 for the N-doped cavity, as most obviously denoted by a higher coherence peak and zero-temperature value of σ_2/σ_n , is likely due to the absence (or lower volume fraction) of proximity coupled nanohydrides and magnetic moments within the interface. This is consistent with the fact that N-doped cavities do not exhibit the high field Q drop caused by the proximity breakdown of hydrides at high fields [7, 10].

Collectively, these findings show that the frequency dip is a hallmark of enhanced Nb SRF cavity performance, as it occurs at the intermediate levels of disorder required for the minimization of the pair-conserving and pair-breaking scattering processes. This, in turn, leads to a larger coherence peak in σ_1/σ_n and an increase in the zero-temperature value of σ_2/σ_n . We thus conjecture that the pair-conserving scattering originates in interstitial impurities that have the beneficial effect of trapping hydrogen.

V. CONCLUSION

This study provides an investigation on the anomalous resonant frequency features that appear just below the critical temperature of Nb SRF cavities and their correlation with several metrics. We find that dilute and uniform concentrations of nitrogen in Nb yield the frequency dip phenomenon and show that the magnitude of this dip is correlated with enhanced superconducting properties, including an increased coherence peak height in AC conductivity and a reduction in surface resistance with increasing RF field. By comparing recently developed theories, we find that these phenomena are driven by an optimal level of impurity scattering, particularly off of nonmagnetic impurities such as nitrogen, which improves cavity performance. The findings suggest that nitrogen doping reduces surface irregularities, such as hydrides and magnetic oxides, which can otherwise impair superconducting performance. Our results not only contribute to the fundamental understanding of superconductivity in niobium but also provide practical guidelines for improving the performance of SRF cavities, with

significant implications for accelerator technologies and quantum systems.

VI. ACKNOWLEDGMENTS

The authors would like to acknowledge O. Melnychuk and D. A. Sergatskov for technical support during measurements. Work supported by the Fermi National Accelerator Laboratory, managed and operated by Fermi Research Alliance, LLC under Contract No. DE-AC02-07CH11359 with the U.S. Department of Energy.

-
- [1] H. S. Padamsee, Superconducting radio-frequency cavities, *Annu. Rev. Nucl. Part. Sci.* **64**, 175 (2014).
- [2] A. Romanenko, R. Pilipenko, S. Zorzetti, D. Frolov, M. Awida, S. Belomestnykh, S. Posen, and A. Grassellino, Three-dimensional superconducting resonators at $T_c < 20$ mk with photon lifetimes up to $\tau = 2$ s, *Phys. Rev. Appl.* **13**, 034032 (2020).
- [3] R. Janish, V. Narayan, S. Rajendran, and P. Riggins, Axion production and detection with superconducting rf cavities, *Phys. Rev. D* **100**, 015036 (2019).
- [4] Z. Bogorad, A. Hook, Y. Kahn, and Y. Soreq, Probing axionlike particles and the axiverse with superconducting radio-frequency cavities, *Phys. Rev. Lett.* **123**, 021801 (2019).
- [5] A. Berlin, R. T. D’Agnolo, S. A. R. Ellis, C. Nantista, J. Neilson, P. Schuster, S. Tantawi, N. Toro, and K. Zhou, Axion dark matter detection by superconducting resonant frequency conversion, *J. High Energy Phys.* **2020**, 88 (2020).
- [6] C. Gao and R. Harnik, Axion searches with two superconducting radio-frequency cavities, arXiv:2011.01350.
- [7] A. Romanenko, F. Barkov, L. D. Cooley, and A. Grassellino, Proximity breakdown of hydrides in superconducting niobium cavities, *Supercond. Sci. and Technol.* **26**, 035003 (2013).
- [8] A. Romanenko, Y. Trenikhina, M. Martinello, D. Bafia, and A. Grassellino, in *Proc. SRF’19* (JaCoW).
- [9] A. Romanenko and D. I. Schuster, Understanding quality factor degradation in superconducting niobium cavities at low microwave field amplitudes, *Phys. Rev. Lett.* **119**, 264801 (2017).
- [10] A. Grassellino, A. Romanenko, D. Sergatskov, O. Melnychuk, Y. Trenikhina, A. Crawford, A. Rowe, M. Wong, T. Khabiboulline, and F. Barkov, Nitrogen and argon doping of niobium for superconducting radio frequency cavities: a pathway to highly efficient accelerating structures, *Supercond. Sci. and Technol.* **26**, 102001 (2013).
- [11] M. P. Garfunkel, Surface impedance of type-i superconductors: Calculation of the effect of a static magnetic field, *Phys. Rev.* **173**, 516 (1968).
- [12] A. Gurevich, Reduction of dissipative nonlinear conductivity of superconductors by static and microwave magnetic fields, *Phys. Rev. Lett.* **113**, 087001 (2014).
- [13] B. Xiao, C. Reece, and M. Kelley, Superconducting surface impedance under radiofrequency field, *Physica C: Superconductivity* **490**, 26 (2013).
- [14] M. Martinello, M. Checchin, A. Romanenko, A. Grassellino, S. Aderhold, S. K. Chandrasekeran, O. Melnychuk, S. Posen, and D. A. Sergatskov, Field-enhanced superconductivity in high-frequency niobium accelerating cavities, *Phys. Rev. Lett.* **121**, 224801 (2018).
- [15] J. Bardeen, L. N. Cooper, and J. R. Schrieffer, Theory of superconductivity, *Phys. Rev.* **108**, 1175 (1957).
- [16] L. C. Hebel and C. P. Slichter, Nuclear spin relaxation in normal and superconducting aluminum, *Phys. Rev.* **113**, 1504 (1959).
- [17] B. Aune *et al.*, Superconducting tesla cavities, *Phys. Rev. ST Accel. Beams* **3**, 092001 (2000).
- [18] H. Padamsee, J. Knobloch, and T. Hays, *RF Superconductivity for Accelerators* (Wiley-VCH Verlag GmbH and Co., KGaA, Weinheim, 1998).
- [19] A. Grassellino, A. Romanenko, Y. Trenikhina, M. Checchin, M. Martinello, O. S. Melnychuk, S. Chandrasekeran, D. A. Sergatskov, S. Posen, A. C. Crawford, S. Aderhold, and D. Bice, Unprecedented quality factors at accelerating gradients up to 45 MVm^{-1} in niobium superconducting resonators via low temperature nitrogen infusion, *Supercond. Sci. Technol.* **30**, 094004 (2017).
- [20] H. Padamsee, *RF Superconductivity: Volume II: Science, Technology and Applications* (Wiley-VCH Verlag GmbH and Co., KGaA, Weinheim, 2009).
- [21] A. Grassellino, A. Romanenko, D. Bice, O. Melnychuk, A. C. Crawford, S. Chandrasekeran, Z. Sung, D. A. Sergatskov, M. Checchin, S. Posen, M. Martinello, and G. Wu, Accelerating fields up to 49 MV/m in tesla-shape superconducting rf niobium cavities via 75C vacuum bake, arXiv:1806.09824.
- [22] D. Bafia, A. Grassellino, O. Melnychuk, A. Romanenko, Z.-H. Sung, and J. Zasadzinski, in *Proc. SRF’19* (JaCoW).
- [23] O. Melnychuk, A. Grassellino, and A. Romanenko, Error analysis for intrinsic quality factor measurement in superconducting radio frequency resonators, *Rev. Sci. Instrum.* **85**, 124705 (2014).
- [24] J. C. Slater, Microwave electronics, *Rev. Mod. Phys.* **18**, 441 (1946).
- [25] J. Halbritter, Institut für Experimentelle Kernphysik (IEKP), Report No. KFK-Extern 03/70-06 (1970).
- [26] M. Martinello, A. Grassellino, M. Checchin, A. Romanenko, O. Melnychuk, D. A. Sergatskov, S. Posen, and J. F. Zasadzinski, Effect of interstitial impurities on the field dependent microwave surface resistance of niobium, *Appl. Phys. Lett.* **109**, 062601 (2016).
- [27] M. R. Trunin, A. A. Zhukov, and A. T. Sokolov, Microwave impedance of $\text{Ba}_{0.6}\text{K}_{0.4}\text{BiO}_3$ crystals: comparison with Nb, *Zh. Eksp. Teor. Fiz.* **111**, 696 (1997).
- [28] G. E. H. Reuter and E. H. Sondheimer, The theory of the anomalous skin effect in metals, *Proc. Roy. Soc. London Ser. A* **195**, 336 (1948).
- [29] W. DeSorbo, Effect of dissolved gases on some superconducting properties of niobium, *Phys. Rev.* **132**, 107 (1963).

- [30] M. Zarea, H. Ueki, and J. A. Sauls, Effects of anisotropy and disorder on the superconducting properties of niobium, *Frontiers in Physics* **11**, 10.3389/fphy.2023.1269872 (2023).
- [31] B. W. Maxfield and W. L. McLean, Superconducting penetration depth of niobium, *Phys. Rev.* **139**, A1515 (1965).
- [32] D. C. Mattis and J. Bardeen, Theory of the anomalous skin effect in normal and superconducting metals, *Phys. Rev.* **111**, 412 (1958).
- [33] R. C. Dynes, V. Narayanamurti, and J. P. Garno, Direct measurement of quasiparticle-lifetime broadening in a strong-coupled superconductor, *Phys. Rev. Lett.* **41**, 1509 (1978).
- [34] P. W. Anderson, Knight shift in superconductors, *Phys. Rev. Lett.* **3**, 325 (1959).
- [35] H. Ueki, M. Zarea, and J. A. Sauls, The frequency shift and q of disordered superconducting rf cavities (2022), arXiv:2207.14236 [cond-mat.supr-con].
- [36] M. Zarea, H. Ueki, and J. A. Sauls, Electromagnetic response of disordered superconducting cavities, *Frontiers in Electronic Materials* **3**, 10.3389/femat.2023.1259401 (2023).
- [37] F. Herman and R. Hlubina, Microwave response of superconductors that obey local electrodynamics, *Phys. Rev. B* **104**, 094519 (2021).
- [38] S. B. Nam, Theory of electromagnetic properties of superconducting and normal systems. i, *Phys. Rev.* **156**, 470 (1967).
- [39] T. Kubo, Effects of nonmagnetic impurities and subgap states on the kinetic inductance, complex conductivity, quality factor, and depairing current density, *Phys. Rev. Appl.* **17**, 014018 (2022).
- [40] N. R. Groll, G. Ciovati, A. Grassellino, A. Romanenko, J. F. Zasadzinski, and T. Proslir, Insight into bulk niobium superconducting rf cavities performances by tunneling spectroscopy, arXiv:1805.06359.
- [41] While PCTS reports higher values of Γ/Δ_0 for both N-doped and EP samples than what is shown in Fig. 5, this is likely due to differences in the probing depth between the two techniques, as PCTS is more surface sensitive and probes regions with more pair-breaking mechanisms.